# Electrochemical and Theoretical Evaluation on the Corrosion Inhibition of Carbon Steel by Organic Selenides in Acidic Medium

*Emad E. El-Katori*[1,*] *and Yasser M. Al Angari*[2]

[1] Department of Chemistry, Faculty of Science (New Valley), Assiut University, El-Kharja 72714, Egypt
[2] Department of Chemistry, Faculty of Science, King Abdul-Aziz University, Jeddah 21589, Saudi Arabia
[*]E-mail: emad_992002@yahoo.com

The influence of organic solenoids as inhibitors for carbon steel (CS) dissolved in 1.0 M HCl had been tested via different electrochemical tests at 298K. Open circuit (OC), Tafel plots, electrochemical impedance spectroscopy (EIS) and electrochemical frequency modulation (EFM) tests had been examined. The gained data had been illustrated that organic selenides functioned as an effective and good inhibitors. The inhibition efficiency (IE%) had been found to improve with improvement of inhibitor concentrations reaching maximum inhibition efficiency more than 80% at 298K. The Tafel plots had been illustrated that the organic selenides coordination were mixed type. The surface morphology of the carbon steel specimens in the absence and presence of organic solenoids had been evaluated by Scanning Electron Microscopy (SEM) and Atomic Force Microscopy (AFM) measurements. The influence of molecular structure on the inhibition efficiency (IE%) has been investigated by quantum chemical computations. The relation between the inhibition efficiency and some quantum parameters have been evaluated and discussed.

## 1. INTRODUCTION

Carbon steel (CS) has been the broaden metal utilized in industrial purpose, Army equipment, building and more in petroleum manufacturing, fertilizers and extra industries. So the carbon steel protection in aqueous solutions is worldwide request, environmental, cheap, and aesthetical important [1]. The inhibitor usage has been more essential way to reduce the carbon steel corrosion. The organic compounds are commonly utilized as corrosion inhibitors as it includes heteroatom for example O and

N atoms. But the organic compounds are hazards and unfriendly environment inhibitors [2]. So the search for alternative friendly environment inhibitors are more important. Carbon steel is an iron alloy, which undertake dissolution smoothly in acid intermediate. Acid, intermediate is commonly applied in synthetically laboratories in addition to various industries like acid cleaning, acid descaling, acid pickling and oil wet cleaning, etc. In other hand CS has been utilized via dissimilar states in chemical and associated industries for acid treating, basic and salt solutions [3]. The organic inhibitors adsorb on metallic surface and then the lower rate of corrosion [4]. It has been noticed that adsorption be controlled largely on definite physicochemical attributes of the inhibitor groups, as electron density, functional groups at donor atoms, π-orbital manner and molecular electronic structure [5-10]. Generally, organic inhibitors having oxygen and/or nitrogen as conjugated double bonds and polar groups in their structures which have been noticed as good corrosion inhibitors for a lot of metallic elements and alloys in different media [11-27]. The organic inhibitors inhibiting job are commonly referred towards their contacts with metallic surfaces via their adsorption. The polarity of functional groups has been considered as the reaction center that settle down adsorption process. On the other hand, the inhibitor adsorption on a metal surface be controlled via scant reasons, for example the nature and surface charge of metal, adsorption manner, the chemical composition of inhibitors and electrolyte solution [28].

Present research will discuss carbon steel dissolution in 1.0 M HCl at 298K in presence of organic selenides via electrochemical techniques. Carbon steel surface specimen morphology has been estimated via SEM and AFM instruments.

## 2. EXPERIMENTAL

### 2.1. Carbon steel sample
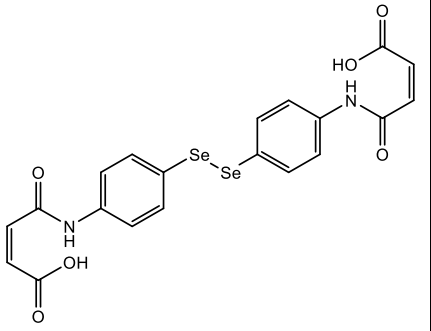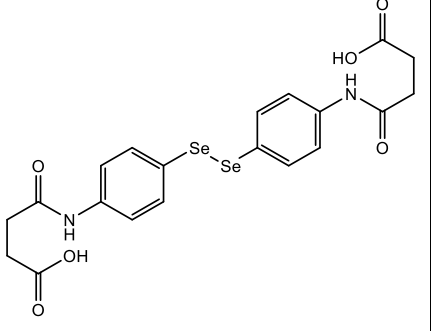
**Table 1.** Carbon steel sample composition:

| Constituent | C | Mn | P | Si | Iron |
|---|---|---|---|---|---|
| Composition (wt. %) | 0.2 | 0.6 | 0.04 | 0.003 | Rest |

### 2.2. Chemicals

### 2.2.1. Inhibitors

Organic selenides had been utilized as inhibitors and described in Table (2). They had been tested and utilized as received [29].

**Table 2.** The Component and molecular structure of the tested inhibitors

| Inhibitor | Structure | IUPAC Name | Molecular weight | Active center | Chemical formula |
|---|---|---|---|---|---|
| **S1** |  | (2Z,2'Z)-4,4'-((diselanediylbis(4,1-phenylene))bis(azanediyl))bis(4-oxobut-2-enoic acid) | 538.28 g/mol | 6O 2N | $C_{20}H_{16}N_2O_6Se_2$ |
| **S2** |  | 4,4'-((diselanediylbis(4,1-phenylene))bis(azanediyl))bis(4-oxobutanoic acid) | 542.31 g/mol | 6O 2N | $C_{20}H_{20}N_2O_6Se_2$ |

### 2.2.2. Solutions

The applicable solution had been 1.0 M HCl, which designed by dilution of analytical grade HCl (37%) with distilled water. The concentrations range of the tested inhibitors had been between ($1 \times 10^{-6}$M and $13 \times 10^{-6}$M).

### 2.3. Electrochemical tests

Electrochemical tests had been achieved by utilizing a cell consists of three electrodes (a) Working electrode, The electrode dimensions are 10 x 10 mm and had been welded from one side of a copper wire used for electric connection and swelled in epoxy resin, to expose geometrical surface areas of 1.0 cm$^2$. This electrode had been abraded as before [30]. (b) Reference electrode had been saturated calomel electrode (SCE), directly utilized with applicable solution, while all potential value had been recorded *vs*. SCE. Lugging-Haber capillary tube had been also involved in the design, Lugging capillary tip had been prepared very close to the working electrode surface reducing IR drop [31]. (c) Platinum wire (1.0 cm$^2$) as auxiliary electrode. All electrochemical tests had been achieved in 1.0 M HCl solution in the absence and presence of different concentrations of organic selenides at 298K under un-stirred and aerated conditions. The tests had been utilized via Potentiostat/Galvanostat/Zera analyzer (Gamry PCI 300/4). This includes Gamry framework system

based on the ESA400, and a personal computer with DC 105 software for potentiodynamic polarization, EIS 300 software for EIS, and EFM 140 software for EFM measurements. Echem Analyst 5.58 software has been utilized for graphing, plotting and fitting data.

### 2.3.1. Open circuit potential (OCP)

The first step in electrochemical experiment. Working electrode had been tested as a function of time during the 10 minutes. This time needful to arrive steady state and gain (OCP) value.

### 2.3.2. Non-destructive method

(a) EIS measurements had been achieved via frequency with range from 0.1 Hz to 100 KHz with amplitude 5.0 mV peak to peak utilizing Ac signals at open circle potential. The empirical impedance had been tested and explicated based on the equivalent circuit. The main parameters derived from EIS test were charge transfer resistance, $R_{ct}$, The capacitance of double layer, $C_{dl}$. Inhibition efficiency (IE %) and surface coverage ($\Theta$) were realized via this equation (1):

$$IE \% = \theta \times 100 = [1-(R°_{ct} / R_{ct})] \times 100 \tag{1}$$

Where $R_{ct}$, $R°_{ct}$ were the charge transfer resistance in the presence and absence of organic selenides, respectively [32-34].

(b) EFM measurements had been achieved by utilizing two frequency 2.0 & 5.0 Hz. Main frequency had been 0.1 Hz, as a result the wave form repeat after 1.0 Sec. Larger frequency must at least two times than the smallest frequency. The larger frequency be required to be appropriately slow that the double layer charging doesn't participate to the current respond. Commonly, 10 Hz reasonable limits. The inter-modulation spectra had been involved current responses allocated for harmony and inter-modulation current peak. Large peaks had been utilized to detect the corrosion current density ($i_{corr.}$), Tafel slopes ($\beta_c$ and $\beta_a$) and causality factors CF-2 & CF-3 [35-36].

### 2.3.3. Destructive method

This method includes DC potentiodynamic polarization techniques which had been utilized to detect corrosion current density under steady state conditions by applying the potential from -1200 to +1200 mV to obtain the Tafel polarization curve and the result current had been plotted as logarithm scale *vs.* potential related to SCE, Extrapolating of two Tafel regions gives ($i_{corr.}$) and ($E_{corr.}$) corrosion potential. By ($i_{corr.}$) we able to calculate the rate of corrosion (R) = 0.13 ($i_{corr.}$) (Equivalent weight) / D where, D= density in $g/cm^3$ [37-40]. Equation (2) was utilized to detect IE% and $\Theta$:

$$IE\% = \theta \times 100 = [1-(i_{corr} / i°_{corr})] \times 100 \tag{2}$$

### 2.4. Surface examination

Carbon steel surface had been getting ready by retaining its coupons for 12 hrs in 1.0 M HCl in the absence and presence of organic selenide inhibitors, after abrading utilizing dissimilar emery

papers up to 2000 grade size after that the coupons had been washed gently with bidistilled water, with awareness dried and mounted into desiccators with no extra treatment. The corroded carbon steel had been inspected by scanning electron microscope (SEM, JSM-T20, Japan) & model Wet–SPM (Scanning Probe microscope) Shimadzu made in Japan had been utilized for AFM tests [41-42].


## 3. RESULTS AND DISCUSSION

### 3.1. Electrochemical tests

#### 3.1.1. Open circuit potential ($E_{OC}$)

Figure 1 be evidence for influence of various concentrations of organic selenide inhibitors on the variation $E_{OC}$ of carbon steel with time in aerated non-stirred 1.0 M HCl solution at 298K. The steady-state value of $E_{OC}$ is larger negative than the inundation potential ($E_{OC}$ at t=0), indicating so as to before the steady state condition has been achieved the pre-inundation, air oxide film formed has to break up [43]. This steady state potential ($E_{corr.}$) which quickly achieved (after about 10 min of inundation), is in contact to the bare metal free corrosion [44]. It has been noticeable that ($E_{corr.}$) shifts to larger negative value without the alteration general feature of E/t plot. On the other hand upon raising the concentration of organic selenides inhibitors.
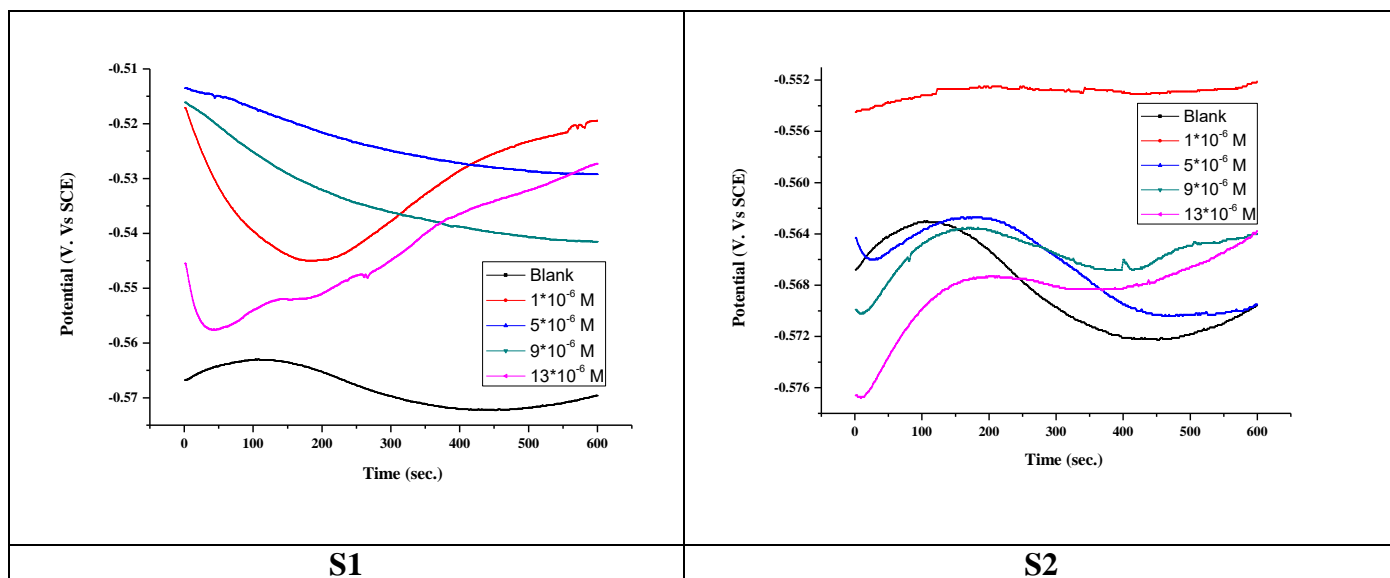


**Figure 1.** Variation of open circuit potential ($E_{OC}$ ) as function of time record for carbon steel in 1.0 M HCl in the absence and presence of different concentrations of organic selenide inhibitors at 298K.

Firstly, the $E_{OC}$ has been proceeding at lower negative potential values, then achieving a maximum one. After assuring time relying on organic selenide  inhibitor concentrations, the potential decrease and arrive a reasonably steady value. These data have been elucidated that two counter-acting processes happened, the first one being a creation of the electrode surface protective adsorbed layer,

and as a result delayed-action corrosion takes place moving the $E_{OC}$ to more noble data. Corrosion has been occurring on the second one, which has been made potential back towards among these two counter-acting operations may possibly elucidate semblance of an arrest or peak in the $E_{OC}$ *vs.* time plot as presented in Figure 1. The steady-state potential proceed towards larger negative values with raising organic selenide inhibitor concentrations. At first $E_{OC}$ shift to lower negative values (as a result of corrosion inhibition) accomplishing higher one, in addition to after assuring the time the potential reduces to accomplish a reasonably steady value (as a result of metal dissolution), causes the steady state corrosion potential to proceed towards larger negative value. These potential data clarify that organic selenides having high efficiency as corrosion inhibitors.
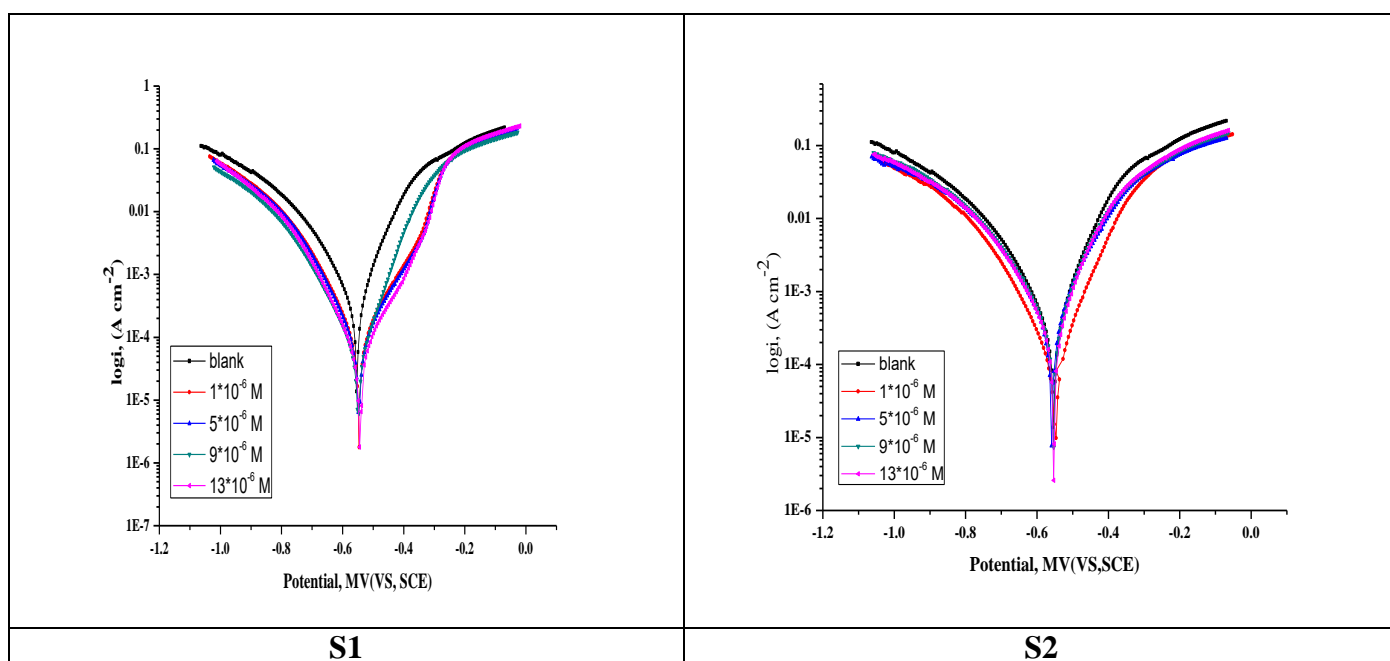
### 3.1.2. Potentiodynamic polarization (PP):



**Figure 2.** Potentiodynamic anodic and cathodic plots of carbon steel in 1.0 M HCl in the absence and presence of different concentrations of organic selenide inhibitors at 298K.

The addition of organic selenides in the tested solution makes a change in PP curves at 298K have been illustrated in Figure 2. The corrosion current densities $i_{corr}$ and the corrosion potentials $E_{corr}$ has been gained at the intersection point from the extrapolation of anodic and cathodic curves. From polarization curves can understand that the addition of organic selenide inhibitors to the tested solution causes no change in the identity of PP curves, but become wider and extrapolated at lower current density, indicating that the inhibitor molecules interfere with reactive sites on metal electrode surface. The PP parameters had been listed in Table 3 indicates that increasing the inhibitor concentrations has been accompanied with a decrease in $i_{corr}$ since the ability of inhibitor molecules has been enhanced to block more reactive sites that are necessary for corrosion reactions [45]. In literature, if the absolute difference in $E_{corr}$ doesn't exceed $\pm 85$ mV, the corrosion inhibitors have been categorized as a mixed type inhibitor as found in this work [46,47]. From the polarization data study, a lower change in $E_{corr}$

values in the presence of corrosion inhibitors, with a maximum difference 16 mV, relative to the $E_{corr}$ obtained from free acid solution. Since the current density in the presence of the organic selenide inhibitors founded S1 has been lower than its parent S2, this means the corrosion inhibition performance of S1 excels its parent S2. The IE% has been obtained from polarization studies and calculated via the subsequent equation (3):

$$IE\% = \frac{i^0_{corr} - i_{corr}}{i^0_{corr}} \times 100 \qquad (3)$$

Where, $i^0_{corr}$, $i_{corr}$ are the current densities acquired from PP measurements in the absence and presence of inhibitors, respectively.

**Table 3.** Electrochemical parameters ($i_{corr}$, $E_{corr}$, $\beta_a$, $\beta_c$ and IE%) associated with polarization tests of carbon steel in1.0 M HCl solution in the absence and presence of different concentrations of organic selenide inhibitors at 298K.

| Inhibitors | Conc.(x10$^{-6}$M) | $i_{corr}$ $\mu A\ cm^{-2}$ | $E_{corr}$ mV | $\beta_a$ mV dec$^{-1}$ | $\beta_c$ mV dec$^{-1}$ | $k_{corr}$ mpy$^{-1}$ | IE% | $\theta$ |
|---|---|---|---|---|---|---|---|---|
| | Blank | 374.0 | -553.0 | 88.8 | 135.50 | 171.00 | ------- | ------ |
| | 1 | 87.5 | -547.0 | 117.6 | 108.20 | 39.98 | 76.6 | 0.766 |
| S1 | 5 | 79.2 | -547.0 | 119 | 107.80 | 36.19 | 78.8 | 0.788 |
| | 9 | 54.7 | -549.0 | 84.1 | 107.70 | 25.00 | 85.4 | 0.854 |
| | 13 | 43.5 | -545.0 | 104 | 97.20 | 19.86 | 88.4 | 0.884 |
| | Blank | 374.0 | -553.0 | 88.8 | 135.50 | 171.00 | ------ | ------ |
| | 1 | 328.0 | -559.0 | 96.6 | 130.90 | 149.70 | 12.3 | 0.123 |
| S2 | 5 | 300.0 | -554.0 | 85.0 | 126.90 | 137.00 | 19.8 | 0.198 |
| | 9 | 211.0 | -553.0 | 75.4 | 114.70 | 96.21 | 43.6 | 0.436 |
| | 13 | 108.0 | -549.0 | 85.2 | 109.20 | 49.22 | 71.1 | 0.711 |

### 3.1.3. EIS measurements

The two main parameters, $R_{ct}$ and $C_{dl}$, have been deduced from electrochemical impedance technique and have been collected in Table 4. In addition, Figure 3 illustrates Nyquist plots & bode plots of carbon steel in the absence and presence of different concentrations of organic selenides in 1.0 M HCl solution.
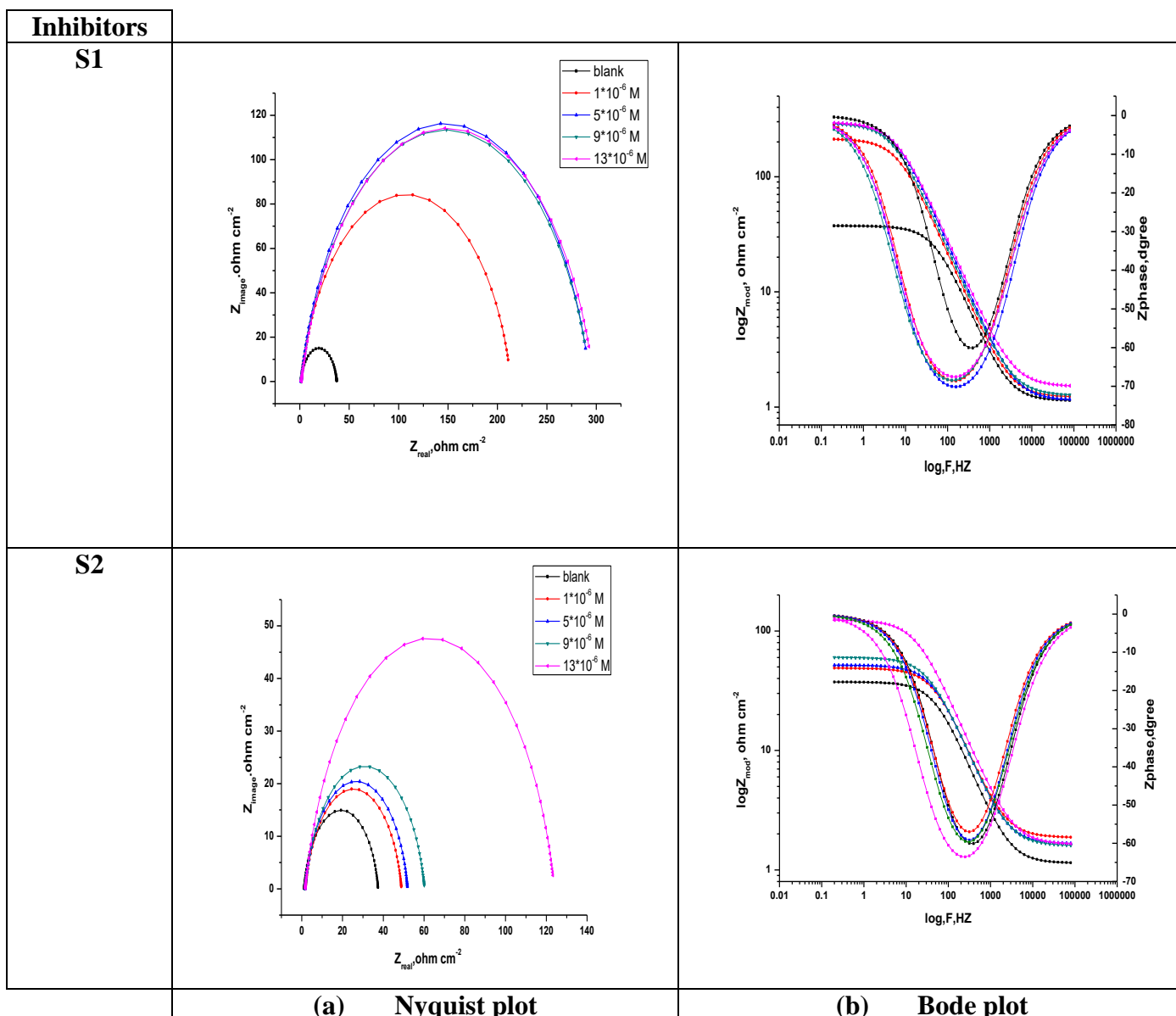
| Inhibitors | | |
|---|---|---|
| **S1** |  |  |
| **S2** |  |  |
| | **(a)    Nyquist plot** | **(b)    Bode plot** |

**Figure 3.** (a) Nyquist and (b) Bode diagrams for carbon steel in 1.0 M HCl containing different concentrations of organic selenide inhibitors at 298K.
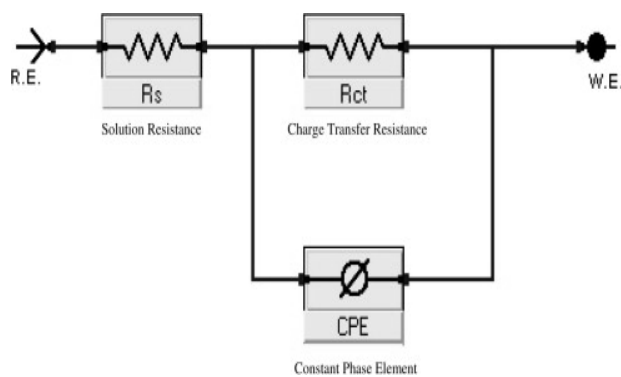


**Figure 4.** An equivalent circuit model for adjusting impedance spectra.

The semicircular nature of impedance graphs point to a charge transmit, process largely manages the carbon steel corrosion, and carbon steel dissolution mechanism stays unaffected when organic selenides have been added to the tested solution [48]. The experimental data have been adjusted to an equivalent electrical circuit, as illustrated in Figure 4, so that the spectral data of Nyquist & bode plots which have been examined. This simulation modeling supports to find out not only the solution resistance $R_s$, but also this can also be useful to predict other important parameters, for example the charge transfer resistance $R_{ct}$ and double layer capacitance $C_{dl}$.

The charge transfer resistance $R_{ct}$ data have been computed from the dissimilarity in impedance at small and large frequencies gained from Bode graphs. $R_{ct}$ values have been regarded as a gauge of electron transfer via carbon steel surface and it is inversely proportional to the rate of corrosion. The capacitance double layer $C_{dl}$ has been computed at the frequency $f_{max}$ at which the unreal module of the impedance has been maximal via the equation (4) [49].

$$C_{dl} = \frac{1}{2\pi f_{max} R_{ct}} \tag{4}$$

The impedance results have been presented in Table (3), indicated that the magnitude of $R_{ct}$ value has been raised while that of $C_{dl}$ has been reduced by adding different concentrations of organic selenides in 1.0 M HCl solution. The lower of $C_{dl}$ data produces from the organic selenide inhibitors adsorption at surface of applicable metal. The double layer among solution and the charged metal surface has been regarded as an electrical capacitor. The organic selenides adsorption on carbon steel surface has been minimized its electrical capacity the same as they exchange water molecules and extra ions adsorbed at the interface surface in order to create a metallic surface protective adsorption layer (working electrode) which raises the width of the electrical double layer. The width of the protective layer ($d$) has been related to $C_{dl}$ in agreement with Helmholtz model, via the subsequent equation (5) [50]:

$$C_{dl} = \frac{\varepsilon \varepsilon_0 A}{d} \tag{5}$$

Where $\varepsilon_o$ is the permittivity of free space ($8.854 \times 10^{-14}$ F/cm), $\varepsilon$ is the medium dielectric constant and $A$ is the electrode effective surface area. Table 6 has been illustrated that, while the width of the protective layer (the film created by inhibitor molecules) raises, the $C_{dl}$ ought to shrink. In this work, $C_{dl}$ data has been found to arrive the maximum for the uninhibited solution. By addition of organic selenides to the applicable acid solution is found to reduce the $C_{dl}$ value. The decrease in $C_{dl}$ values by raising organic selenide inhibitors concentrations via the reduction of the surface coverage blocked by the action of creating an interface adsorbed layer surface among the acid solution and the metal. The inhibition efficiency of organic selenides for carbon steel dissolved in 1.0 M HCl has been computed via $R_{ct}$ values from the subsequent equation (6):

$$\% IE = \theta \times 100 = [1 - (R^{\circ}_{ct}/R_{ct})] \times 100 \tag{6}$$

The $R_{ct}$ and $\theta_{max}$ values have been raised by raising the organic selenide concentrations, while $C_{dl}$ values tend to reduce. It is well known that the capacitance is inversely proportional to the width of double layer [50]. A small capacitance may be via water molecules at the electrode interface are largely substituted by corrosion inhibitor molecules through the adsorption [51]. The larger inhibitor molecule also reduces the capacitance through raising in the double layer width.

**Table 4.** Impedance parameter numerical values (Rs, $R_{Ct}$, $C_{dl}$, $\theta_{max}$ and IE%) associated with impedance tests of carbon Steel in 1.0 M HCl solution in the absence and presence of different concentrations of organic selenide inhibitors at 298K.

| Inhibitors | Conc. (x10$^{-6}$M) | $R_{ct}$ | $C_{dl}$ μF | IE% | $\theta$ |
|---|---|---|---|---|---|
| **S1** | Blank | 37.71 | 193.0 | --------- | ------- |
| | 1 | 212.70 | 6.75 | 82.3 | 0.823 |
| | 5 | 292.30 | 3.96 | 87.1 | 0.871 |
| | 9 | 292.50 | 3.80 | 87.1 | 0.871 |
| | 13 | 295.90 | 3.70 | 87.3 | 0.873 |
| **S2** | Blank | 37.71 | 193.0 | ------- | ------- |
| | 1 | 47.10 | 139 | 19.9 | 0.199 |
| | 5 | 50.25 | 129 | 25.0 | 0.250 |
| | 9 | 58.66 | 95.4 | 35.7 | 0.357 |
| | 13 | 122.20 | 22.0 | 69.1 | 0.691 |

The protective layer width has been raised by raising the organic selenide concentrations, since more protonated inhibitor molecules will electrostatic adsorb on the electrode surface wrapped with negative layer. This process results in a noticeable reduction in $C_{dl}$ this trend is in accordance with Helmholtz model, via the subsequent equation (7):

$$C_{dl} = \frac{\varepsilon \varepsilon_\circ A}{d} \tag{7}$$

Where d, is the protective layer width, $\varepsilon$ is the medium dielectric constant, $\varepsilon_\circ$ is the vacuum permittivity and A is the effective electrode surface area. The $R_{ct}$ values have been utilized to compute IE% values via the subsequent equation (8):

$$IE\% = 100 \times \theta = 100 \times \left[\frac{R_{ct} - R_{ct}^\circ}{R_{ct}}\right] \tag{8}$$

Where $R_{ct}$ and $R_{ct}^\circ$ are the charge transfer resistance of inhibited & uninhibited solutions, correspondingly. As a result, the inhibition efficiency raised by raising inhibitor concentrations.

### 3.1.4. EFM tests

Electrochemical frequency modulation (EFM) has been the non-destructive corrosion method that is able to provide data of the corrosion current in the absence of known data of Tafel constant directly. Like EIS, it's a low signal Ac method not similar to EIS, on the other hand two sine waves (at different frequencies) are tested for cell jointly. For the reason that current has been non-linear potential function of the system respond in non-linear route to potential excitation. The current response involves not only the enter frequencies, but also involve frequency compositions which are the total, variation and multiples of the two input frequencies. The two frequencies cannot be selected at haphazard. They be required to be low, integer multiples of a base frequency that detect the length of the method. Figure 5 Shows representative examples for inter-modulation spectra which have been achieved by EFM tests. Every spectrum has been a current response as a frequency function. The two

high peaks, with amplitudes of about 100μA, have been the response of the 2.0 Hz and 5.0 Hz excitation frequency. Peaks among 1.0 μA & 20 μA have been the harmonics, totality and diversity of the two excitation frequencies. These peaks have been utilized by EFM140© software package to compute corrosion current and Tafel constants. It is most important to note that among the current response peaks is very low. There has been nearly no response (<100nA) at 4.5 Hz, as, they are a direct effect of the EFM method [52-53].
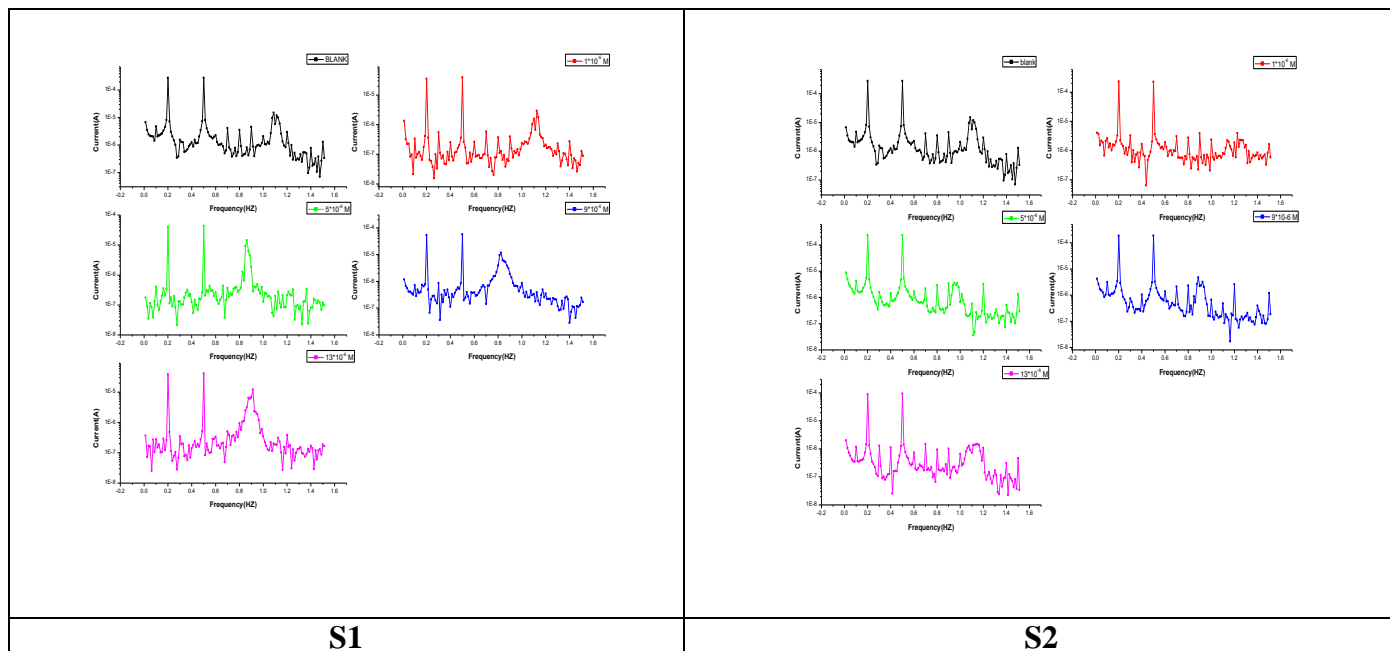


**Figure 5.** Inter-modulation spectrum recorded for carbon steel in 1.0 M HCl in the absence and presence of different concentrations of organic selenide inhibitors at 298K and at respective corrosion potential.

Corrosion kinetic parameters have been recorded in table 7 are computed from EFM technique, utilizing the subsequent equations (9-13):

$$i_{corr} = \frac{i_\omega^2}{\sqrt{48(2i_\omega i_{3\omega} - i_{2\omega})}} \tag{9}$$

$$\beta_a = \frac{i_\omega U_\circ}{2i_{2\omega} + 2\sqrt{3}\sqrt{2i_{3\omega} i_\omega - i_{2\omega}^2}} \tag{10}$$

$$\beta_c = \frac{i_\omega U_\circ}{2\sqrt{3}\sqrt{2i_{3\omega} i_\omega - i_{2\omega}^2 - 2i_{2\omega}}} \tag{11}$$

$$\text{Causality factor (2)} = \frac{i_{2\omega 2 + \omega 1}}{i_{2\omega 1}} = 2.0 \tag{12}$$

$$\text{Causality factor (3)} = \frac{i_{2\omega 2 + \omega 1}}{i_{3\omega 1}} = 3.0 \tag{13}$$

Wherever i, is the instantaneous working electrode current density measured at frequency ω and $U_0$ is the sine wave distortion amplitude. Table 5. Illustrated corrosion kinetic parameters such as inhibition efficiency (IE %), corrosion current density ($i_{corr}$), Tafel constants ($\beta_a$, $\beta_c$) and causality factors (CF-2, CF-3) as an inhibitor concentration function in presence and non presence of inhibitors.

It's clear that $i_{corr}$ values, reduce while IE% raise with the raising of inhibitor concentrations. IE% were computed from equation (14):

$$IE\% = \theta \times 100 = \left(1 - \frac{i_{corr}}{i^{\circ}_{corr}}\right) \times 100 \qquad (14)$$

Where $i^{\circ}_{corr}$ and $i_{corr}$ are corrosion current density in the absence and presence of inhibitors, respectively.

**Table 5.** The electrochemical kinetic parameters of EFM test for carbon steel in 1.0 M HCl in the absence and presence of different concentrations of organic selenide inhibitors at 298K and at respective corrosion potential.

| Inhibitors | Conc.(x $10^{-6}$M) | $j_{corr.}$, $\mu A\ cm^2$ | $\beta_a$, V $dec^{-1}x10^{-3}$ | $\beta_c$, V $dec^{-1}x10^{-3}$ | CF-2 | CF-3 | IE% | $\theta$ |
|---|---|---|---|---|---|---|---|---|
| **S1** | Blank | 412 | 93.89 | 99.73 | 1.69 | 3.20 | ------- | ------ |
| | 1 | 71.35 | 116.70 | 130.9 | 2.30 | 2.70 | 82.7 | 0.827 |
| | 5 | 57.86 | 88.02 | 90.95 | 1.98 | 3.50 | 86.0 | 0.860 |
| | 9 | 55.3 | 64.10 | 66.49 | 2.03 | 3.40 | 86.6 | 0.866 |
| | 13 | 30.44 | 49.10 | 50.75 | 1.76 | 3.07 | 92.6 | 0.926 |
| **S2** | Blank | 412 | 93.89 | 99.73 | 1.69 | 3.20 | ------ | ----- |
| | 1 | 375 | 100.90 | 110.2 | 1.58 | 3.05 | 9.0 | 0.090 |
| | 5 | 351.3 | 93.94 | 98.49 | 1.79 | 3.30 | 14.7 | 0.147 |
| | 9 | 281.3 | 96.23 | 100.8 | 1.69 | 3.04 | 31.7 | 0.317 |
| | 13 | 151.3 | 102.60 | 113.6 | 1.58 | 2.70 | 63.3 | 0.633 |

The large intensity of EFM is causality factor which provide as an internal try on the EFM test's validity [51]. By means of the causality reasons the experiential EFM values can be confirmed. In table 5 causality factors have been in agreement with two theoretical values according to the EFM method [50]. Must warranty the validity of tafel constants and corrosion current densities. The CF-2 and CF-3 standard values are 2.0 and 3.0, respectively [50]. It is quite evident that the electrochemical tests gained data are compatible with the EFM tests gained data.
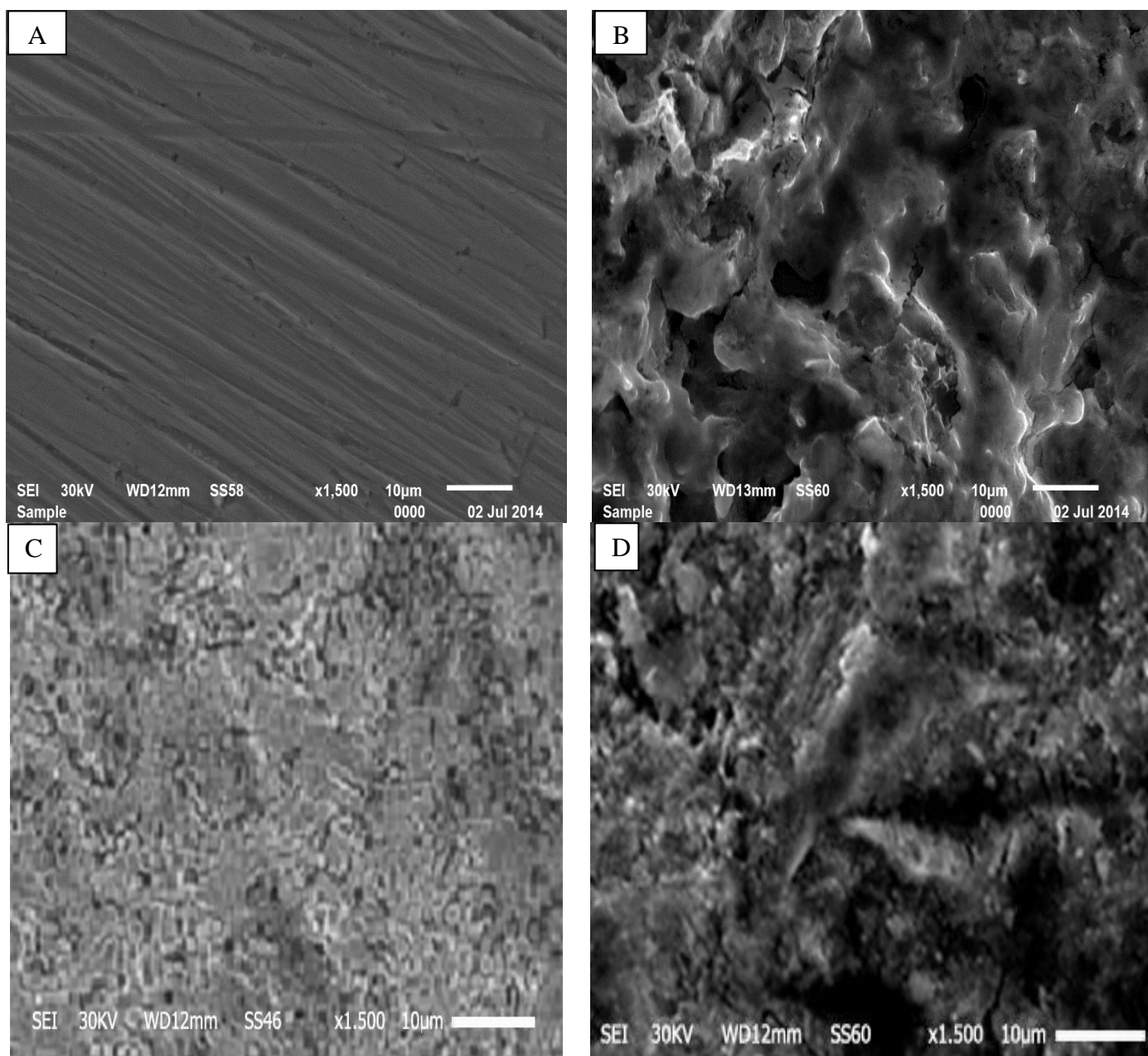
*3.2 Scanning Electron Microscope (SEM)*



**Figure 6.** SEM graphs of carbon steel surface (A) before inundation in 1.0M HCl, (B) after 12 h of inundation in 1.0M HCl (C) after 12 h of inundation in 1.0 M HCl + 13X10$^{-6}$M of S1 (D) after 12 h of inundation in 1.0M HCl + 13X10$^{-6}$M of S2 at 298K.

Figure 6 illustrates SEM graphs for surface of carbon steel alone and after 12 hour inundation in aerated 1.0 HCl solution in the absence and presence of 13X10$^{-6}$M of organic selenide inhibitors. As expected (A) be evidence for clarity of metallic surfaces, (B) in the absence of inhibitor, carbon steel surface has been damaged by aerated 1.0 M HCl solution, while (C&D) in the presence of organic selenide inhibitors, the metallic surface seems to be nearly non influenced by acid medium [54].
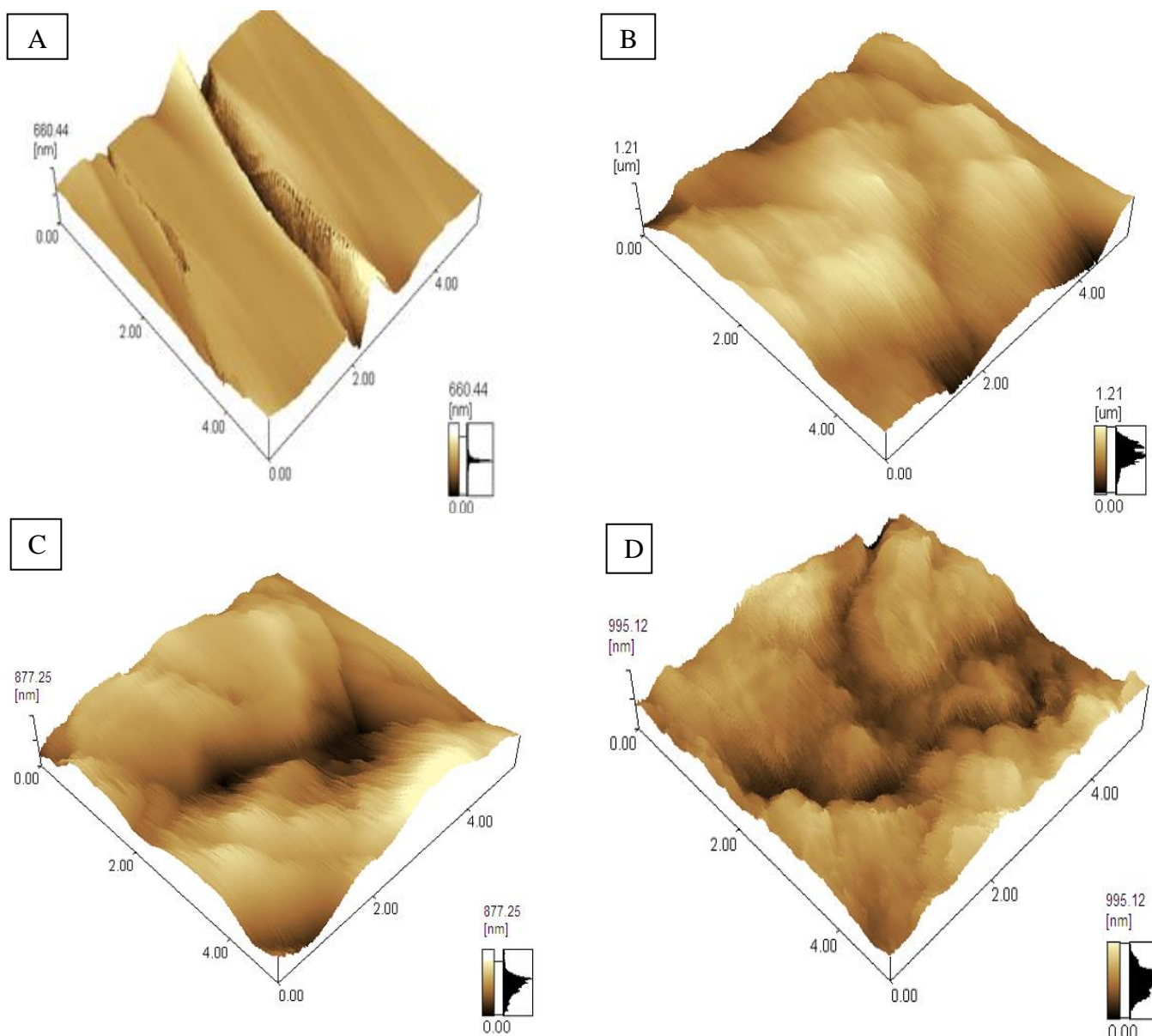
*3.3 Atomic Force Microscopy (AFM)*



**Figure 7.** AFM graphs of carbon steel surface (A) before inundation in 1.0M HCl, (B) after 12 h of inundation in 1.0M HCl (C) after 12 h of inundation in 1.0 M HCl + 13X10$^{-6}$M of S1 (D) after 12 h of inundation in 1.0M HCl + 13X10$^{-6}$M of S2 at 298K.

The roughness of carbon steel surface by utilizing organic selenides inhibitors have been given in the absence and presence of 13X10$^{-6}$M organic selenide inhibitors by AFM maximum-resolution; the outcome data are shown in Figure 7, continually. The outcome data from both in the absence and presence of organic selenide inhibitors, the roughness of surface ($R_{max}$) data = 680.44 nm, 1210 nm, 877.25 nm and 995.12 nm, continually. The data of $R_{max}$ lower with presence of organic selenides to the medium, led to that the film covered deposited in the presnce of organic selenides provide a reduce in roughness via formation of an adsorbed organic selenide films on carbon steel surface [55].

### 3.4 Quantum chemical calculations

The computational calculation parameters have been gained via DFT theory in order to clarify the corrosion inhibition characteristics of the tested organic compounds and elucidate the inhibition mechanism in terms of electronic and molecular structure properties, like $E_{HOMO}$, $E_{LUMO}$, energy gap $\Delta E = E_{LUMO} - E_{HOMO}$ and dipole moment ($\mu$) have been scheduled in Table 8. Frontier molecular orbital's (FMO$_s$) supply with the greater part to the chemical reactivity of organic molecules, especially the Highest Occupied Molecular Orbital (HOMO) and the Lowest Unoccupied Molecular Orbital (LUMO).The metal and inhibitors interaction via the electron donation from inhibitors occupied orbital's (mainly from the HOMO) to d-orbital of metal [56], together with through the electrons acceptance from the d-orbital of metal to unoccupied orbital's (mainly to the LUMO ) of the inhibitor. As a result, the LUMO energy ($E_{LUMO}$) is a sign of the potency of molecule to gain electrons; the more negative the value of $E_{LUMO}$, the molecule more possible to gain electrons [57]. There have been parallel relationships have been informed between the inhibition efficiency (IE%) and the energy gap ($\Delta E$) in the (FMOs) ($\Delta E = E_{LUMO} - E_{HOMO}$). Therefore, the larger $E_{HOMO}$ value & the lower the $E_{LUMO}$ value, the more ability of inhibitor molecules to adsorb on metal surface, which gives rise to better corrosion inhibition efficiency. The binding ability of inhibitors to metal surface raises with raising of $E_{HOMO}$ and reducing of $E_{LUMO}$ values. Frontier molecular orbital diagrams of DMOPP are illustrated in Figure 8. The energy gap ($\Delta E_{L-H}$) is a significant parameter as a function of reactivity of inhibitor molecules in the direction of adsorption on the metal surface. As $\Delta E_{L-H}$ reduces the reactivity of the molecule raises driving to better inhibition efficiency [58].

**Table 8.** The quantum chemical parameters computed for the tested inhibitors via the DFT method in the neutral and cationic form of inhibitors.

| Inhibitors | $E_{HOMO}$ | $E_{LUMO}$ | $\Delta E$ (eV) | Pi (eV) | X | $\eta$(eV) | $\sigma$ (eV) | $\mu$ | Dipole Debye |
|---|---|---|---|---|---|---|---|---|---|
| S1 | -9.25 | -3.80 | 5.45 | -6.525 | 6.525 | 2.73 | 0.367 | -3.65 | 6.130 |
| S2 | -9.24 | -3.75 | 5.49 | -6.495 | 6.495 | 2.75 | 0.364 | -3.79 | 6.930 |

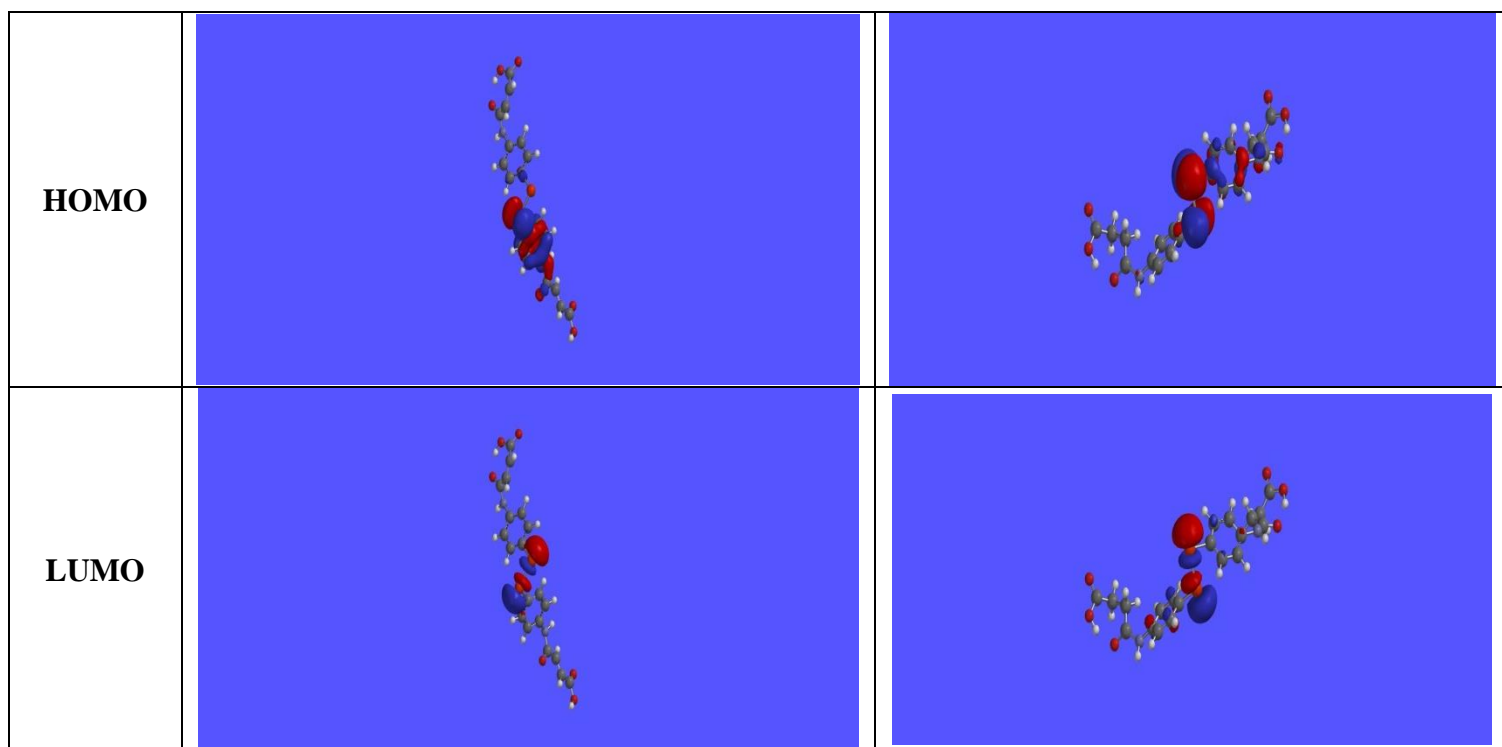| Inhibitors | S1 | S2 |
|---|---|---|
| **Optimized structures** |  |  |
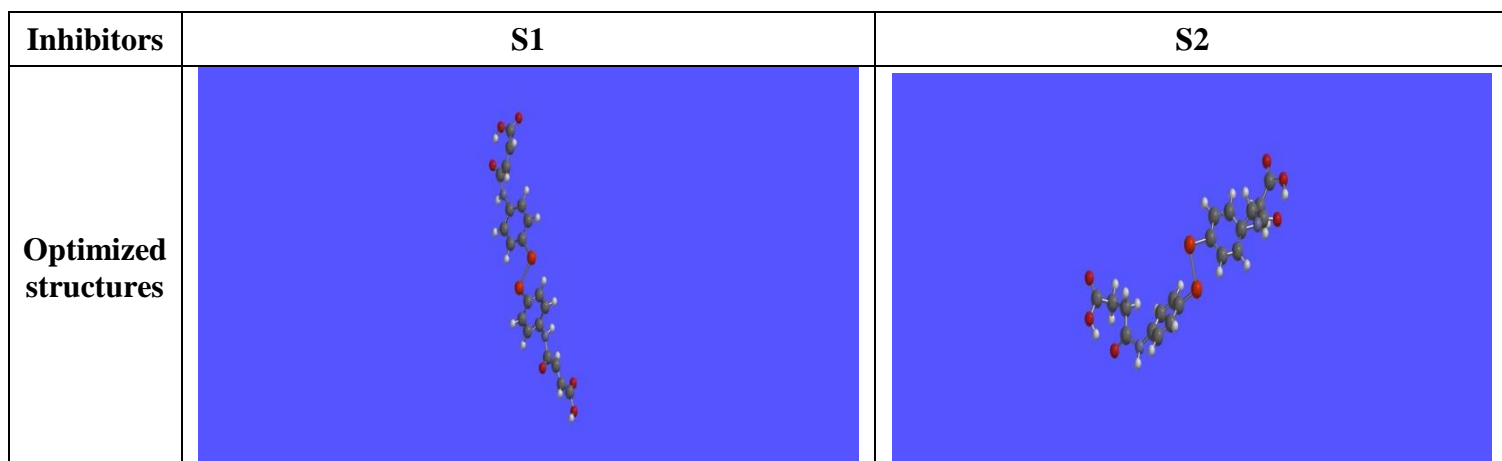
**Figure 8.** The optimized structure, HOMO and LUMO distribution of molecules of organic selenide compounds.

The dipole moment ($\mu$) is another significant electronic parameter provided for non-uniform sharing of charges on the different atoms in the molecule. The larger value of dipole moment (6.2) in Table 8, probably raises the adsorption among the inhibitor and the metal surface. The deformability energy rises with raising in ($\mu$), as a result the molecule facile to adsorb on the iron surface. As well, the inhibitor molecules volume also raises with raising ($\mu$), this raise the contact area among the iron molecule and surface, raising the corrosion inhibition ability of inhibitors [59].

*3.5 Mechanism of Inhibition*

Corrosion inhibition of carbon steel in 1.0 M HCl solution via organic selenide inhibitors have been tested by OCP, PP, EIS and EFM methods; it has been found that the %IE depends upon inhibitors concentrations, metal nature, the adsorption manner of inhibitors and surface setting. The experimental corrosion data in the presence of these inhibitors are as follows: (i) decrease in corrosion rate (CR) and corrosion current with raising organic selenides inhibitor concentrations, (ii) the shift in Tafel lines to larger potential sections and (iii) %IE depending on the number of adsorption active centers in the molecule and their charge density. It is included that the manner of adsorption depends on the attraction of the metal en route for the p-electron clouds of the ring system. Metals such as Fe, which have a greater attraction en route for aromatic moieties, have been found to adsorb benzene rings in a flat orientation. The studied organic selenides inhibitors exhibited good inhibition efficiencies in corrosive solution have been as follows: S1>S2 due to the carboxylic acid groups are

directed to the metal surface in case of S1 due to restricted rotation around the double bond; whereas, in case of S2 there is free rotation around the sigma bond and therefore the carboxylic groups may undergo rotation far from the metal surface, as well as  Fe metal surface has  been carried positive charge, chloride ions (Cl⁻) may be first adsorbed onto the metal surface positively charged. After that, the inhibitor molecules adsorb via electrostatic interactions between organic selenides positively charged molecules and the metal surface negatively charged and create a protective layer [60,61].
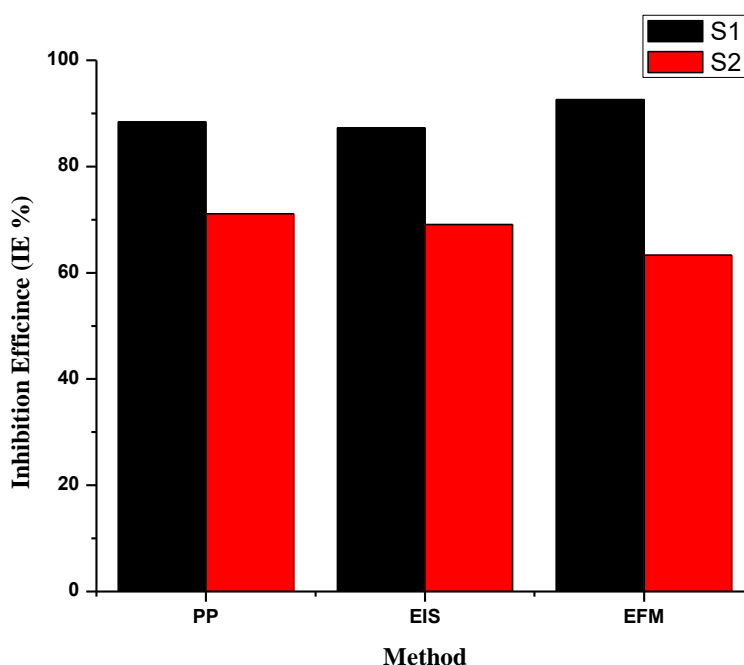
## 4. CONCLUSIONS



**Figure 9**. Comparison of IE% resulted  from experimental methods for corrosion of carbon steel in 1.0 M HCl containing $13 \times 10^{-6}$ M of the testing organic selenides inhibitors at 298K.

Polarization, Impedance, EFM, SEM and AFM have been utilized in order to study the corrosion inhibition of carbon steel in 1.0 M HCl via corrosion inhibitors " organic selenides ". The major conclusion is:

1- The corrosion process reduces strongly with organic selenides and IE% raised with rising organic selenide concentrations in this order S1>S2.
2- The open circuit potential has been more positive with raising organic selenide inhibitor concentrations.
3- The corrosion current reduces with raising organic selenide inhibitor concentrations.
4- The $R_{ct}$ and $\theta_{Max.}$ Values have been raised with rising organic selenide inhibitor concentrations, while $C_{dl}$ reduces.

The inhibition efficiency data resulted from the spolarization, impedance and EFM methods are compatible with each other.

## References

1. I.   Al-shafey, M. A. Abass, A. A. Hassan, S. A. Sadeek, *IJABC*, 3 (2014) 1004.
2. O. A. Hazazi, A. Fawzy, M. Awad, *Int. J. Electrochem. Sci.*, 9 (2014) 4086.
3. A. A. Farag, I. M. Ibrahim, *IJSR*, 3 (2014) 1087.
4. S. Kshama Shetty, A. Nityananda, Shetty, *Canadian Chemical Transactions*, 3 (2015) 41.
5. S.T. Arab and E.A., Noor, *Corrosion*, 49 (1993) 122.
6. I. A. Raspini, *Corrosion*, 49 (1993) 821.
7. N. Hajjaji; I. Ricco, A. Srhiri, A. Lattes, M. Soufiaoui, A. Benbachir, *Corrosion*, 49 (1993) 326.
8. M. Elachouri, M.S.  Hajji, M. Salem,  S. Kertit, R. Coudert, E.M. Essassi, *Corros. Sci.*, 37 (1995) 381.
9. H. Luo, Y.C. Guan, K.N. Han, *Corrosion*, 54 (1998) 619.
10. M.A. Migahed, E. M. S. Azzam, A.M. Al-Sabagh, *Mater.Chem.Phys.*, 85 (2004) 273.
11. M.M. Osman, A.M. Omar, A.M. Al-Sabagh, *Mater.Chem.Phys.,* 50, 271- 274, (1997).
12. F. Zucchi, G. Trabanelli, G. Brunoro, *Corros. Sci.,* 33 (1992) 1135.
13. R.F.V. Villamil, P. Corio, J.C. Rubim, M.L. Siliva Agostinho, *J.Electroanal.Chem.*, 472 (1999) 112.
14. T.P. Zhao, G.N. Mu, *Corros.Sci.,* 41 (1999) 1937.
15. S.S. Abd El Rehim, H. Hassan., M. A. Amin, *Mater.Chem.Phys.,* 70 (2001) 64.
16. S.S. Abd El Rehim, H. Hassan., M. A. Amin, *Mater.Chem.Phys.,* 78 (2003) 337-348.
17. R. Guo, T. Liu, X. Wei, *Colloids Surf. A*, 209 (2002) 37-45.
18. V. Branzoi, F. Golgovici, F. Branzoi, *Mater.Chem.Phys.,* 78 (2002) 122-131.
19. R. Oukhrib, B. El Ibrahimi, H. Bourzi, K. El Mouaden, A. Jmiai, S. El Issami, L. Bammou, L. Bazzi, *JMES*, 8 (2017) 195.
20. A. M. Al-Azzawi, K. K. Hammud,  *IJRPC*, 6 (2016) 391.
21. L. El Ouasif, I. Merimi, H. Zarrok, M. El ghoul, R. Achour, M. Guenbour, H. Oudda, F. El-Hajjaji and B. Hammouti, *J. Mater. Environ. Sci.,* 7  (2016) 2718.
22. U. M. Sani and U. Usman,  *International Journal of Novel Research in Physics Chemistry & Mathematics*, 3 (2016) 30-37.
23. A.M. Kolo, U.M. Sani, U. Kutama and U. Usman, *The Pharmaceutical and Chemical Journal*, 3 (2016) 109.
24. P. O. Ameh and U. M. Sani, *Journal of Heterocyclics*, 1 (2015) 2.
25. H. I. Al-Shafey, R. S. Abdel Hameed, F. A. Ali, A. S. Aboul-Magd, M. Salah, *Int. J. Pharm. Sci. Rev. Res.*, 27 (2014) 146.
26. R. Kushwah and R. K. Pathak, *International Journal of Emerging Technology and Advanced Engineering,* 4 (2014) 880-884.
27. A. S. Fouda, M.N. EL-Haddad and Y.M.Abdallah, *IJIRSET*, 2 (2013) 7073.
28. S. U. Ofoegbu  and P. U. Ofoegbu, *ARPN Journal of Engineering and Applied Sciences*,7 (2012) 272.
29. Saad Shaaban, Amr Negm, Abeer M. Ashmawy, Dalia M. Ahmed, Ludger A. Wessjohann, *European Journal of Medicinal Chemistry,* 122 (2016) 55-71.
30. K. Shalabi, Y. M. Abdallah, Hala M. Hassan and A. S. Fouda, *Int. J. Electrochem. Sci.*, 9 (2014) 1468.
31. Y. M. Abdallah, Hala M. Hassan, K. Shalabi and A. S. Fouda, *Int. J. Electrochem.* Sci., 9 (2014) 5073.
32. A. S. Fouda, G. Y. Elewady, K. Shalabi and H. K. Abd El-Aziz, *RSC Adv.*, 5 (2015) 36957.
33. M. A. Hegazy, Ahmed Abdel Nazeer, K. Shalabi, *Journal of Molecular Liquids*, 209 (2015) 419.
34. Abd El-Aziz S. Fouda, Emad E. El-Katori and Saedah Al-Mhyawi, *Int. J. Electrochem. Sci.*, 12 (2017) 9104 – 9120.
35. K. Shalabi, Y. M. Abdallahm A. S. Fouda, *Res Chem Intermed.*, 41 (2015) 4687.

36. A. H. El-Askalany, S. I. Mostafa, K. Shalabi, A. M. Eid, S. Shaaban, *Journal of Molecular Liquids,* 223 (2016) 497.
37. A. S. Fouda, K. Shalabi and A. A. Idress, *Int. J. Electrochem. Sci.,* 9 (2014) 5126.
38. A. S. Fouda, K. Shalabi, G. Y. Elewady and H. F. Merayyed, *Int. J. Electrochem. Sci.,* 9 (2014) 7038.
39. A.S. Fouda, A.A. Al-Sarawy, E.E. El-Katori, *Desalination,* 201 (2006) 1.
40. Abd El-Aziz Fouda, Ahmed Al-Sarawy and Emad El-Katori, *European Journal Chemistry,* 1 (2010) 312.
41. Abd El-Aziz S Fouda, Safaa H Etaiw, M Hammouda, *Journal of Bio-and Tribo-Corrosion,* 3 (2017) 29.
42. A. S. Fouda, M.Eissa, G. Y. Elewady, W.T. El behairy, *Int. J. Electrochem. Sci.*, 12 (2017) 9212 – 9230.
43. M. Bouanis, M. Tourabi, A. Nyassi, A. Zarrouk, C. Jama, F. Bentiss, *Applied Surface Science*, 389 (2016) 952.
44. A. S. Fouda, T. Fayed, M. A. Elmorsi, M. Elsayed,  *J Bio Tribo Corros*. 3 (2017) 33.
45. A. S. Fouda, A. M. El- Defrawy and M. W. El-Sherbeni, *J. Applicable  Chemistry*, 39 (2012)  1.
46. M. A. Chidiebere, C. E. Ogukwe, K. L. Oguzie, C. N. Eneh and E. E. Oguzie, *Ind. Eng. Chem. Res.*, 51 (2012) 668.
47. Y. Qiang, S. Zhang, S. Xu and W. Li, *J. Colloid Interface Sci.,* 472 (2016) 52.
48. A. Y. Musa, A. B. Mohamad, A. A. H. Kadhum, M. S. Takriff and L. T. Tien, *Corros. Sci*., 53 (2011)  3672.
49. L. Hu, S. Zhang, W. Li and B. Hou, *Corros. Sci.,* 52 (2010) 2891.
50. A. Kosari, M. H. Moayed, A. Davoodi, R. Parvizi, M. Momeni, H. Eshghi and H. Moradi, *Corros. Sci.,* 78 (2014) 138.
51. A. Biswas, S. Pal and G. Udayabhanu, *Appl. Surf.  Sci*., 353 (2015) 173.
52. Mohammed A. Amin; M.A. Ahmed, H.A. Arida, Taner Arslan, Murat Saracoglu and Fatma, *Corros. Sci,.*, 53 (2011) 540.
53. R.W. Bosch, and W.F. Bogaerts, *Corrosion*, 52 (1996)  204.
54. A.K. Singh, M.A. Quraishi, *Corros.Sci*, 53 (2011) 1288.
55. B. Wang, M. Du, J. Zhang, C.J. Gao, *Corros.Sci*, 53 (2011) 353.
56. A. Y. Musa, A. A. H. Kadhum, A. B. Mohamad, A. A. B. Rahoma , H. Mesmari, *Journal of Molecular Structure,* 969 (2010) 233.
57. E. S. H. El Ashry, A. El Nemr, S. A. Esawy, S. Ragab, *Electrochimica Acta,* 51 (2006) 3957.
58. R. M. Issa, M. K. Awad and F. M. Atlam, *Applied Surface Science*, 255 (2008) 2433.
59. X. Li, S. Deng, H. Fu and T. Li, *Electrochimica Acta*, 54 (2009) 4089.
60. I.B. Obot, N.O. Obi-Egbedi and S.A. Umoren, *Corros. Sci.*, 51 (2009) 1868.
61. A. K. Singh and M. A. Quraishi, *Corros. Sci.*, 52 (2010) 152.